Zn-AgCl paper-based battery as an ionic conductivity sensor

Author: Oriol Juan Sabater
Facultat de Física, Universitat de Barcelona, Diagonal 645, 08028 Barcelona, Spain.

Advisor: Juan Marcos Fernández Pradas, Susana Liébana Girona (CNM)

Abstract: We present a novel single-use Zn-based self-powered battery unit design for ionic conductivity sensing. Three devices have been fabricated in order to assess changes in reproducibility and performance based on geometrical variables. This work reports the design, fabrication, test and analysis of the mentioned devices.

I. INTRODUCTION

Point of Care Devices (PoC) aim to bring medical technology closer to the patient. These devices encompass a wide range of tests, from COVID-19 and pregnancy tests to on-site laboratory diagnostics. They offer multiple advantages such as transportability, simplicity, rapid diagnosis and reduced costs.
However, most PoC devices rely on the patient's interpretation, which can introduce ambiguities on the reading. To address this challenge, the scientific community has been actively working on its digitalization. Apart from providing an accurate result this also holds the potential to enable data tracking of the population, leading to a more efficient healthcare system.

Many existing solutions for the digitalization of PoC devices involve complex systems, with many electronic components. Since the majority of the tests are single-use devices they exhibit challenges such as their environmental impact or an elevated cost-functionality ratio.

Within this context, the SPEED Group (CNM) proposed a paper-based electrochemical self-powered battery sensor for the quantification of conductivity. [1] This paper introduces a novel approach whereby the energy generated through the electrochemical reactions of the electrodes serves as a direct measure of the activation solution's conductivity, eliminating much of the complexity associated to classical AC conductimetric methods.
The practical implementation of this technology has been successfully demonstrated in previous studies focused in the assessment of athletes' dehydration and the screening of Cystic Fibrosis disease. [2]
However, in prior devices, magnesium (Mg) was employed as the anode material. Despite its advantages in terms of a higher reaction potential and capability to perform on neutral media, the use of Mg posed limitations due to its unsuitability for printing processes because of its high reactivity or the presence of a relatively thick native oxide layer on its surface. [3]

Following SPEED's line of research, this work provides an overview of the design, development, characterization and optimization of a novel Zn-based battery unit. The battery will be used to detect viral nucleic acid by Loop-mediated isothermal amplification (LAMP) experiments, in which a decrease in conductivity of the samples takes place when the viral ARN is amplified [4]. The incorporation of Zn in the design will facilitate the adoption of printable inks, thereby enhancing the repeatability and scalability of results in a large-scale production. It will also minimize activation losses attributed to the presence of a native oxide layer in the anode. [5]

II. SETUP AND METHODS

A. Self-powered conductivity sensor operation

In order to employ the battery unit as a self-powered conductometer it is necessary to set its operation within the region of ohmic losses (see figure 1 (A)), where its voltage output is directly proportional to the internal resistance of the battery.

As noted in [1], the internal resistance comprises several components:

- Faradaic Resistance (R_F). It is associated to the activation losses produced by the native oxide layer of the electrodes. Since it is quickly removed, this element will solely be significant at low voltages.
- Ohmic Resistance (R_O). Associated to the ohmic resistance of the electrodes and electrical contacts, it is constant for a specific configuration of our system.
- Ionic resistivity of the electrolyte (R_I). It is influenced both by the paper bridge characteristics (such as porosity or geometry) and the solution's conductivity.

Consequently, if both the ionic bridge and the setup remain unchanged, variations in the device's internal resistance are attributed merely to variations of the activation solution's conductivity, thereby affecting the slope of the characteristic I-V curve. This effect is the keystone for the implementation of a self-powered battery conductivity sensor.

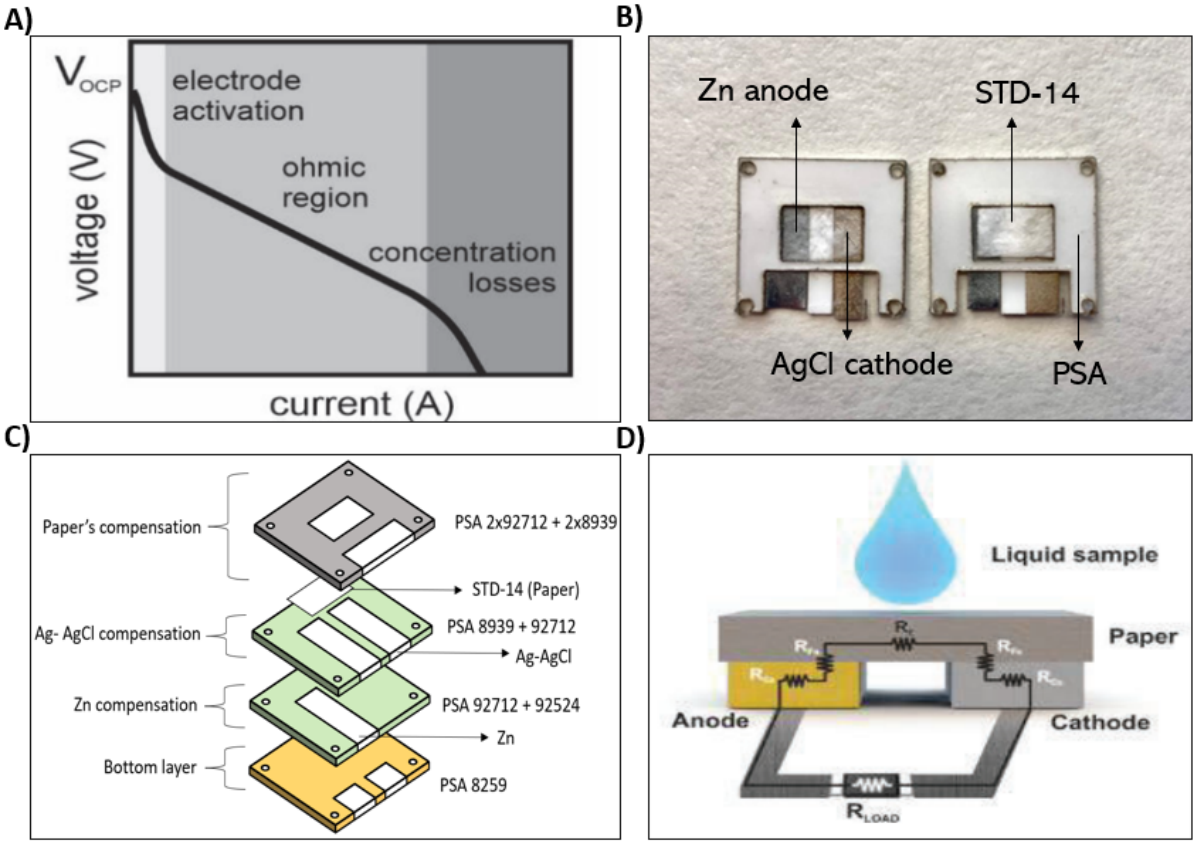

FIG. 1: (A) I-V polarization curve depicting the different current regions. Reprinted with the permission of [6] (B) Battery units after testing (C) Overview of the structural configuration of the proposed paper-based battery sensor (D) Scheme depicting the different contributions to the internal resistance of the battery. Reprinted with permission of [7]

B. Methods and materials

A primary battery functions by converting electrochemical potential energy into electrical energy. In this model the energy is generated through the integration of two distinct redox (Reduction-Oxidation) reactions of opposite sign, interconnected by an ion-conducting medium. The underlying chemical reaction taking place within the battery can be described as follows:

$$\mathrm{Zn(s) + 2\,AgCl(s) \longrightarrow Zn^{2+}(aq) + 2\,Ag + 2\,Cl^{-}(aq)}$$

The cathode undergoes reduction by gaining electrons. We have opted for AgCl as the cathode material due to its broad range of printable inks alternatives, reactivity and price.

By means of the screen-printing technique, which involves manually applying mechanical force to transfer ink through a mesh and evenly distribute it to create complex patterns, we have fabricated a two layer cathode. The bottom Ag layer is designed to facilitate electron flow. The top AgCl layer is where the desired chemical reaction occurs.

Commercially available inks, namely Silver Chloride C16003P7/211112902 (60/40 Ag/AgCl) and Silver 2022182/0224016380, have been employed for this purpose.

The anode is made out of Zn foil. As mentioned before, in future phases of the project the goal is to use Zn ink, so it can be screen-printed to increase repeatability.
The open circuit potential is expected at around 1V [8].

An important component when designing the battery is the ionic bridge employed to connect the two electrodes. Dissociated ions from the ionic solution help balance out the charge imbalances generated by the electron flow during the redox reaction, in accordance to the principle of charge conservation. Therefore, this element will be critical in determining the ionic resistance of the battery, and consequently its performance.

During the fabrication process, Standard 14 (STD-14) paper has been employed due to its widespread availability and cost-effectiveness. This paper is typically

	Area (mm^2)	Distance (mm)
Model 1 (reference)	10	2,5
Model 2	10	1,5
Model 3	12,5	2,5

TABLE I: Summary of the different fabricated designs.

employed in comercial lateral flow tests since it has a high degree of porosity and very low reactivity with biological samples. Its placement in the device can be seen in Figure 1 (B).

As shown in Figure 1 (C), the battery unit consists of two electrodes, anode and cathode, separated by a certain distance. To ensure the stability and proper positioning of each electrode component, Pressure Sensitive Adhesive (PSA) layers of varying thickness and materials have been employed, depending on its thickness. Both papers and PSA components have been cut using an Epilog Laser cutter.
All the pieces have been mounted on top of a Poly(methyl methacrylate) (PMMA) platform with four lateral alignment pins to help the correct manual placement.

The schematic in this image depicts the structure of the battery. It comprises four primary layers, each with a specific functionality.

1. The lowermost layer serves as the platform for accommodating all the battery components.
2. The Zn and Ag-AgCl compensation layers equalize the height disparity between the Zn electrode and the Ag-AgCl electrode. This ensures effective contact between the ionic bridge and the electrodes.
3. The uppermost layer secures the placement and stability of the STD-14 paper.

To optimize the battery sensor unit, three distinct models have been developed in order to assess two design variables, such as the spacing between electrodes and the active area (see Table I for further details). These models aim to evaluate the sensor's sensitivity to conductivity changes.

The experimental procedure aimed to characterize performance with at least three replicates for each conductivity of the activation solution, a dilution of NaCl with varying molarities. A consistent volume of 25 μl was employed for each trial.

III. RESULTS

In this section, a comparative analysis will be conducted on the different fabricated battery units, with a particular focus on assessing their variations in relation to geometry.

Concentration (mM)	σ (mS·cm $^{-1}$)
100	8.854
50	4.625
25	2.396
12.5	1.22
6.25	0.6175

TABLE II: Conductivities of NaCl dilutions at different concentration. Measured with the pH/conductometer Metrohm 6.0917.080

Figure 2 displays the obtained experimental results. Images (A,B) offer a direct comparison of the polarization curves between the reference model (model 1) with model 2 (reduced inter-electrode distance, $d = 2,5mm$) and model 3 (increased area, $A = 12.5mm^2$).
Results in Figure 2 (A) clearly indicate that reducing the distance between electrodes leads to a decrease in the ionic resistance of the paper bridge. Consequently, the current lines density traversing between the electrodes exhibit an increase in magnitude, allowing for a wider range of currents to be achieved with the same voltage drop. Notably, there is a substantial increase in power density output, nearly doubling the standard value.
In contrast, Figure 2 (B) demonstrates that increasing the electrode area produces a decrease in the overall density of current lines. Based on these results, we can conclude that current lines originating from regions distant from the center contribute less to the total current, which leads to an overall decrease of the current density. The maximum power density curve will also be reduced.

The results presented provide evidence that the distance between the electrodes is one of the critical geometric variable influencing the performance of the sensing unit. Among the models examined, Model 2 is the one yielding the best performance in terms of output power.

Figure 2 (C) depicts the polarization curve of Model 2 at various NaCl concentrations (see table II for the corresponding conductivities). To utilize the battery unit as a sensor, a straightforward approach involves connecting it in series with an external resistive load (R_{LOAD}). The voltage output of the unit for a specific activation solution concentration can be determined by the intersection of R_{LOAD} with the polarization curves.

The voltage output at a specific conductivity, V_σ, can be described as:

$$V_\sigma = \frac{V_{OCP} \cdot R_{LOAD}}{R_\sigma + R_{LOAD}} \tag{1}$$

Where V_{OCP} is the Open-Circuit Potential, R_σ is the internal resistance of the battery and R_{LOAD} is the connected external resistor. In this configuration, the delivered voltage will depend upon the internal

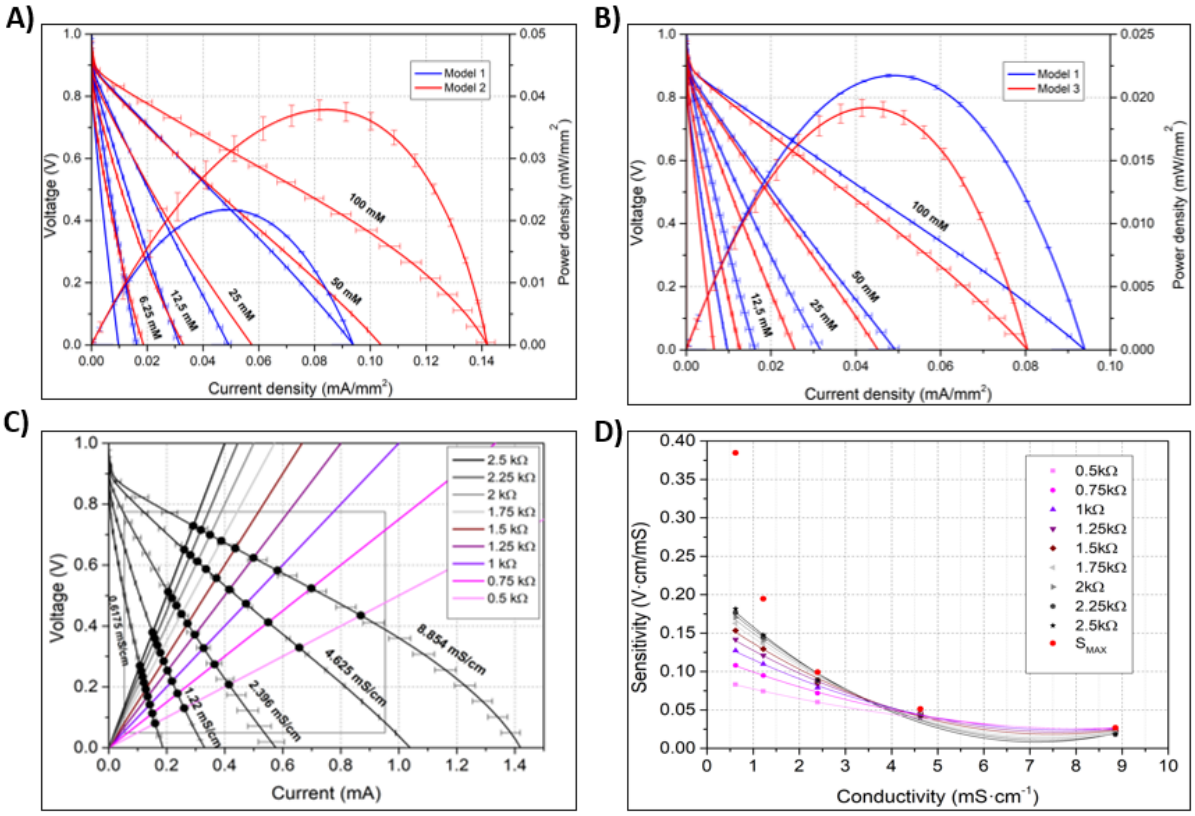

FIG. 2: (A) j-V characteristic polarization curve of model 1 and 2. Curves range from lower to upper values of concentration in ascending order for both devices. Highest power density output curves are also displayed for each model (B) j-V characteristic polarization curve of model 1 and 3. Highest power density output curves are also displayed for each model (C) I-V characteristic polarization curve of model 2 intersecting a range of resistive external loads. Each dot corresponds to the intersection between both curves and is directly proportional to the internal resistance of the battery (D) Model 2 sensitivities for different external resistive loads and conductivities. The theoretical S_{MAX} is depicted the red.

resistance, whilst the resistive load will modulate the battery response. Detailed calculations can be found in literature [1].

In this same image, I-V characteristics of R_{LOAD} ranging from $0.5k\Omega$ to $2.5k\Omega$ have been superposed to the battery I-V polarization curves.

When comparing these batteries to the work presented in [1], it becomes apparent that the applicable spectrum of this battery is significantly broader. The obtained activation voltage drop is approximately $\Delta V \approx 0,1V$ while it is reported to be $\Delta V \approx 0,33V$ in previous Mg-based batteries. Concentration losses are only manifested in Model 2 at higher current levels.

The sensitivity of the battery can be expressed as [1]

$$S = \frac{\partial V_\sigma}{\partial R_\sigma}\frac{\partial R_\sigma}{\partial \sigma} = \frac{-V_{OCP}R_{LOAD}}{(R_\sigma + R_{LOAD})^2}\frac{\partial R_\sigma}{\partial \sigma} \qquad (2)$$

Figure 2 (D) displays the sensitivity of the sensor at different conductivities and R_{LOAD} together with the theoretical S_{MAX}. As expected, at low conductivities we will have the greatest sensitivity.
The battery unit will perform fairly well as a sensor for low to mid concentration solutions, but will not be as good for higher conductivities (above 5 mS/cm). Note that for low-mid conductivities, a higher resistive load presents higher sensitivity, whilst for higher conductivities it is the opposite.

From equations we can derive that S_{MAX} at different conductivities, σ, will be achieved by connecting an R_{LOAD} that matches the internal resistivity of the battery for that specific σ. This means R_{LOAD} will be a key parameter for a functional implementation of the device.

Moreover, with the assumption that the ohmic resistance of the electrical contacts, R_O, is minimized so R_I is dominated by the electrolyte resistivity, S_{MAX} can be expressed as follows:

$$S_{MAX} = \frac{V_{OCP}}{4\sigma} \qquad (3)$$

Experimental data satisfies the above equation for mid to high conductivites, but differ in the lower spectrum. Since the R_{LOAD} required to match the theoretical S_{MAX} does not seem feasible we can deduct that ohmic losses play an important role in that range.

It has been proven that the implementation of a Zn cathode achieves similar performance in terms of sensitivity along the whole range of conductivites compared to [1]. It also achieves similar S_{MAX} despite this parameter's dependence with V_{OCP}.
Moreover this device increases in reproducibility because of the thinner oxide passivating layer in Zn and the lower sensitivity to Cl^- ions concentration of the sample.

IV. CONCLUSIONS

This paper presents a novel self-powered paper-based battery unit model for conductivity sensing. By using a Zn-based anode, the model represents a first approximation leading the way to an increase of reproducibility and scalability of future designs with the incorporation of Zn-based ink.
An optimization process have been conducted with two different models in order to determine key geometric variables for performance. Distance have been found to have the greatest impact on power output.

This paper has conducted experiments analysing the behaviour of current lines in the horizontal plane. In future steps it will be necessary to test the model with multiple paper-based bridge layers, in order to assest the effect on current lines in the vertical plane.

Results display promising results in terms of sensitivity to changes for low to medium conductivities, providing similar outcomes to previous works but with a much broader range of available sensing region. The proposed design also offers great reproducibility, which is a key parameter for an optimized sensor performance.

Future work will be directed towards the implementation of a fully-printed battery unit and its application to sense viral presence with nucleic acid amplification techniques.

Acknowledgments

I would like to thank Dra.Susana Liébana and predoctoral fellow Aida Visús for their unconditional help at all times and their willingness to always lend me a hand. I am also grateful for the great insights provided by Dra. Neus Sabaté.

[1] Ortega,L., Llorella, A., Esquivel, J.P, Sabaté, N. Paper-Based Batteries as Conductivity Sensors for Single-Use Applications ACS Sensors 2020 5 (6), 1743-1749 DOI: 10.1021/acssensors.0c00405

[2] Ortega, L., Llorella, A., Esquivel, J.P. . Self-powered smart patch for sweat conductivity monitoring. Microsyst Nanoeng 5, 3 (2019). https://doi.org/10.1038/s41378-018-0043-0

[3] Wang, S., Wang, Y., Ramasse, Q. et al. The Nature of Native MgO in Mg and Its Alloys. Metall Mater Trans A 51, 2957–2974 (2020). https://doi.org/10.1007/s11661-020-05740-1

[4] Zhang, X., Liu, W., Lu, X., Gooding, J., Li, Q., Qu, K. Monitoring the progression of loop-mediated isothermal amplification using conductivity. Analytical Biochemistry 466 (2014) 16–18. https://doi.org/10.1016/j.ab.2014.08.002.

[5] Chen, Y., Schneider, P. and Erbe, A. (2012), Investigation of native oxide growth on zinc in different atmospheres by spectroscopic ellipsometry. Phys. Status Solidi A, 209: 846-853. https://doi.org/10.1002/pssa.201100542

[6] Ortega Tañá, L. Paper-based bateries as key-enablers for self-powered conductivity sensing. May 19 2021. http://hdl.handle.net/2445/177999

[7] Bares, K. A; Anderson, M. L. Stofan, J. R.; Dalrymple, K. J.; Reimel, A. J.;Roberts, T. J.; Randell, R. K.; Ungaro, C. T.; Baker, L. B. Normative Data for Sweating Rate, Sweat Sodium Concentration, and Sweat Sodium Loss in Athletes: An Update and Analysis by Sport. Journal of Sports Sciences.June 22,2019. pp. 2356-2366. https://doi.org/10.1080/02640414.2019.1633159

[8] Heakal, F., Abd-Ellatif, W., Tantawy, N., Taha, A.. Impact of pH and temperature on the electrochemical and semiconducting properties of zinc in alkaline buffer media. RSC Advances. (2018). 8. 3816-3827. 10.1039/C7RA12723E. DOI: 10.1039/C7RA12723E